Thermodynamic description of condensed phases

Bernhard Wunderlich

Abstract Phases may be smaller than visible to the human eye. In order to characterize a *microphase*, a phase smaller than 1 μm, one must consider surface area and free energy in addition to the standard thermodynamic functions. As one approaches nanometer sizes, one also needs to know the changing thermodynamic functions within the phases. The Gibbs–Thomson equation can be used to characterize microphases, but not nanophases. For the latter, the glass transition is needed to assess the properties in the interior. In order to classify condensed phases as *liquid*, *solid*, *mesophase*, or *crystal*, one needs to consider the molecular motion in addition to the molecular structure. Most important are *large-amplitude* displacements in form of translation, rotation, and conformational motion. An *operational definition* based on experiments and an updated classification of the phases is given. The surprising result is the observation that crystals, earlier assumed prime examples of solids, can have order–disorder transitions to more mobile mesophases, as well as a glass transition without change in crystal structure, i.e., under certain condition, they cannot be identified as a solid. To these observations, one has to add the fact that large-amplitude motion may start gradually to a more mobile phase without abrupt changes in structure. These observations limit the usefulness of the 80-year-old classification of transitions as being of first or second order. Quantitative thermal analysis is shown to be an important tool to identify the possible total of 57 different condensed states in terms of their macroscopic properties as well as molecular structure and motion.

Keywords Phase · Molecular motion · Disordering transition · Glass transition · Rigid-amorphous fraction · Nanophase

B. Wunderlich
Department of Chemistry, The University of Tennessee,
Knoxville, TN 37996-1600, USA

B. Wunderlich (✉)
200 Baltusrol Rd, Knoxville, TN 379234-37-7, USA
e-mail: Wunderlich@CharterTN.net

Introduction

As a first step, an improved description is given in this article for the term *phase*. Traditionally, a phase is assumed to be a macroscopic, homogeneous object. In the light of the following discussion, such phase would be called a *macrophase*. As the size of the phase becomes smaller than visible to the human eye, the phase boundaries have an increasing influence on its properties. For a full description of *microphases*, defined as phases smaller than about 1 μm in at least one dimension, one must consider surface area and free energy in addition to the bulk properties of the interior of the phase. As one approaches phases of nanometer size, it is insufficient to know only bulk and surface properties [1]. In *nanophases*, the enthalpy, density, and related properties in the interior of the phase change as a function of their position relative to the surface [2] never reaching the bulk properties of the macrophase [1]. For the understanding of the thermodynamic functions of nanophases one, thus, needs to know the changes of the calorimetric functions within the phase, a completely new concept in the thermodynamics of phase descriptions. The Gibbs–Thomson equation was used for many years to evaluate the increasing surface free energy of increasingly smaller microcrystals via the decrease in melting temperature [3–7]. Thermodynamically this surface free energy is

the only additional quantity distinguishing a microphase from a macrophase. For nanocrystals, additional information must be gathered. The glass transition, linked to the change in molecular motion on a nanometer-scale, can be used to assess the varying interior with their position in the nanophases [6, 7].

As a second step in the phase description, one usually classifies the condensed phases as *liquids*, *solids*, or *mesophases*. This links their molecular structure to their mechanical appearance. Since in the past, no scientific definitions were given to distinguish liquids from solids, one normally utilizes their imprecise dictionary description [8]. In order to resolve the confusion caused by keeping the historic dictionary terms for scientific classifications, one must consider molecular motion in addition to structure. For this purpose, it is convenient to divide molecular motions into those of small and large amplitudes. The small-amplitude motion is represented by vibrations. The large-amplitude motion depends on the molecular structure and may consist of translation, rotation, and internal rotations (also called conformational motion). Large-amplitude motions typically have picosecond time scales (ps) when they occur as local motions and, in case of cooperative motion, they slow to macroscopic time scales (milliseconds to days). Based on thermodynamics, structure, and motion, an *operational definition* [9] for the phases is possible. The molecular structure can be determined by X-ray and electron diffraction, supported by latent heat information. The changes in large-amplitude motion can be deduced from IR spectroscopy and solid-state NMR, the loss tangent, and deviations of heat capacity from their vibrational values. The thermodynamic analysis of phases and their changes can be based on the understanding of the glass transition and the disordering transitions.

Based on such experiments, an updated classification of the phases was shown in Fig. 1 [10]. The surprising result from analyzing a multitude of different substances is the observation that crystals, earlier described as prime examples of solids, may in some cases not only have disordering transitions to more mobile, partially ordered mesophases, but also a glass transition without a change in crystal structure. This means that some crystals are not solid at all as marked in Fig. 1, on the left by a possible internal glass transition. To these observations, one has to add the fact that the usually more abrupt change of crystal structure to a mobile mesophase may start gradually with local, large-amplitude motion at a much lower temperature. These observations limit the usefulness of the early classification of transitions as being of first or second order [11]. Quantitative thermal analysis will be shown to be an important tool to improve the understanding of phases in terms of macroscopic properties as well as microscopic molecular structure and mobility [6, 7].
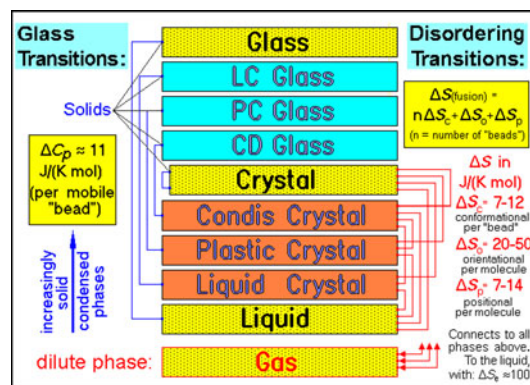

Fig. 1 A classification of phases and their transitions, based on molecular structure and large-amplitude motion

Phase description

Thermodynamically a phase is "a state of matter that is uniform throughout, not only in chemical composition, but also in physical state. In other words, a phase consists of a homogeneous, macroscopic volume of matter, separated by well-defined surfaces of negligible influence on the phase properties" [12]. Domains of a sample which differ in composition or physical states are considered to be different phases. The basic elements of phases are their atoms, as linked to molecules. They set the limit of homogeneity within a phase. This phase definition applies to macrophases and must be distinguished from microphases and nanophases. The differences of the properties of the three phases are of special importance for the understanding of semicrystalline macromolecules and for nanophases in general. A schematic of the three phase sizes is shown in Fig. 2, with details to be discussed in the next section.

The dictionary descriptions for the classical phases, marked in Fig. 1 by the dotted background, were established a long time ago. Merriam-Webster's Collegiate Dictionary [8], for example, suggests that a *solid* is "a substance that does not flow perceptibly under moderate
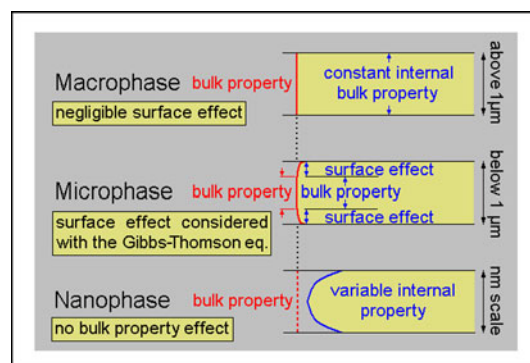
Fig. 2 Schematic sketch of the effect of different phase dimensions on the properties within the phases

stress, has a definite capacity for resisting forces (as compression or tension) which tend to deform it, and under ordinary conditions retains a definite size and shape." Looking for a definition of the *glass*, also considered a solid, one finds as the dictionary description "an amorphous material formed from a melt by cooling to rigidity without crystallization." A *liquid*, in turn, "is a fluid (as water) that has no independent shape but has a definite volume and does not expand indefinitely and that is only slightly compressible." The *gas*, finally also described as a fluid (as seen in air) and "has neither independent shape nor volume but tends to expand indefinitely." For common use, these descriptions are sufficient, but phrases in the description of the solid such as "does not flow perceptibly, moderate stress, definite capacity, and ordinary conditions," and, of the liquid and gas, such as "indefinitely and slightly" are imprecise as long as one does not set specific limits. In order to improve on these definitions, one might want to use *operational definitions* as suggested by Bridgman [9], i.e., one should look for quantitative experiments (operations) as they are discussed in the later sections. On the base of these operations, one should be able to answer the question whether a given substance is a gas, liquid, solid, mesophase, crystal, or glass. A final dictionary meaning is given for the word *transition*. It is to be a "passage from one state, stage, subject, or place to another" [8], in the present discussion, from one phase to another.

The gas at the bottom of Fig. 1 is characterized as a dilute phase, all others are condensed phases and become increasingly solid in the upward direction. The transitions governing the changes to solids are marked on the left and labeled as glass transitions. This makes the measurement of the glass transition temperature, T_g, the operation defining a solid. Below T_g, a phase is a solid, one of the upper five phase boxes, with a dividing line somewhere in the frame of the crystal, often at the bottom line. Above T_g, a phase is one of the lower condensed phases. The disordering transitions on the right side of Fig. 1 determine the changes of entropy (measured via the latent heats). The glass and disordering transitions are discussed in more detail in the later sections. The stages of the development that ultimately led to the present, new Fig. 1 is documented sequentially in the references of [14, 15], [10], and [6].

Phase sizes

The importance of microphases, defined in the previous section and represented in the schematic of Fig. 2, was already noted by Gibbs in his "Theory of Capillarity." He stated that the "influence of surfaces of discontinuity upon the equilibrium of heterogeneous masses" must be considered [12, 13], a detailed microphase thermodynamics is

given in [16]. Two observations are easily linked to surface effects. One is the existence of *colloidal particles* with typical sizes of less than 1 μm. In the frame of the present discussion, these particles (or droplets) are microphases. Colloids are kept in metastable dispersion by surface properties (for example, charges) which prohibit coagulation which would lead to a smaller surface area and, thus, more stability. The other observation is a lowering in the melting temperature of microcrystals due to the (positive) free energies of the surfaces.

About 20 years ago, it became customary to use the term *nanophase* for smaller microphases [1, 2]. This, naturally, requires a separate operational definition for nanophases. It was recognized that these "small microphases" differ in property from "large microphases." This change in property was already suggested by Richard Feynman in 1959. He speculated that "on a small scale we will get an enormously greater range of possible properties that substances can have" [17].

For flexible, semicrystalline macromolecules, it was observed even earlier that small, disordered entities exist which are larger than point defects in crystals, but smaller than microphases. Initially, we called these defects *amorphous defects* [3]. Ultimately, it became clear that the amorphous defects behave like very small phases with a different T_g than a microphase. Based on phase transitions of small and large molecules newly measured and collected from the literature, an *operational definition of nanophases* was suggested which distinguishes them from microphases on the basis of their properties: "In nanophases, the opposing surfaces of a phase area are sufficiently close to interact" [1].

While a microphase is described as a phase with a sufficiently large surface area to cause changes from the macrophase, it can still be considered a bulk phase, enveloped by a distinct surface layer of higher free energy. Only the surface layer, characterized by changes in mass density, mobility, order, and force-field, has different properties from the bulk it encloses. The *nanophase*, in contrast, with its interacting surfaces, has *no* remaining bulk phase in its interior. In addition, the surface layer is known to change gradually in its properties from top to bottom. In nanophases, thus, one expects a continuous change in its properties from the outside to the center of the phase without reaching the plateau of the macrophase, as shown in Fig. 2. The operation to distinguish a nanophase from a microphase, thus, must involve the detection of the internal properties of the phase. If there is bulk phase remaining inside the phase, it is a microphase (or even a macrophase), if not it is a nanophase. An experiment suited for this operation is the measurement of the glass transition since the glass transition is fixed by the properties of volume elements of dimensions of 1 nm or less [6, 7].
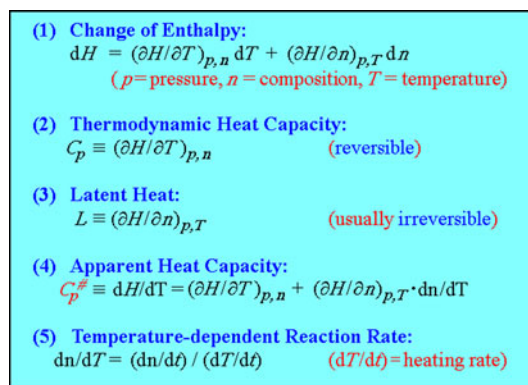
In 1963, structures of the size of approximately 1 nm were suggested to account for certain defects in semi-crystalline fibers [18]. These defects were similar to the amorphous defects proposed at the same time [3, 19] and were later shown to be nanophases, as mentioned above. In such nanophases, single, flexible macromolecules which may reach lengths of more than 100 μm may cross phase boundaries multiple times. *Semicrystalline polymers* are, thus, globally metastable aggregates of more than one of the phase types of Fig. 1 and the phases may be sufficiently small to be nanophases.

In order to characterize a material, one must know which of the phases listed in Fig. 1 are present and then specify their sizes and interconnections (couplings). In addition, the *class of the molecules* may be of importance. After flexible, linear macromolecules had been recognized by Staudinger in the 1920s [20, 21], it became obvious that there exist only three distinct classes of molecules, *small molecules*, *flexible macromolecules*, and *rigid macromolecules* [5, pp 4–5]. This classification scheme is linked to the possible phase properties of the molecules [10]. Rigid macromolecules can only exist as solids. On liquefaction or evaporation, the strong bonds linking the atoms of the molecules are broken, destroying the molecular integrity. Flexible macromolecules can be disordered without losing their integrity, so that for many, liquid as well as solid states are possible (but not gaseous states). Small molecules, under proper conditions, finally, may exist in all three states. Examples of all three molecule classes are found in each of the historically defined inorganic, organic, and biological molecules. The traditional separation of molecule types is, thus, less useful to understand the properties of matter.

The description of the 10 phases given in Fig. 1, the 3 phase-sizes of Fig. 2, and the just reviewed three classes of molecules may be combined in 90 different ways. Gases, however, must be of small molecules and because of the lack of self-sustaining surfaces cannot be microphases or nanophases. Rigid macromolecules, in turn, may not become liquids or mesophases. Finally, mesophases are often coupled to specific molecule types, leaving only 57 *different condensed states* [1].

Determination of phase properties by thermal analysis

Calorimetry is the main tool to measure thermodynamic properties [6, 7]. The differential change in *enthalpy* (heat content), dH, at constant pressure as a function of changing temperature, dT, and composition, dn, is measured by the heat flow into or out of a sample, as given in Eq. 1 of Fig. 3. The enthalpy of many compounds has been determined with adiabatic calorimetry. As long as the phase

(1) Change of Enthalpy:
$$dH = (\partial H/\partial T)_{p,n}\, dT + (\partial H/\partial n)_{p,T}\, dn$$
(p = pressure, n = composition, T = temperature)

(2) Thermodynamic Heat Capacity:
$$C_p \equiv (\partial H/\partial T)_{p,n} \qquad \text{(reversible)}$$

(3) Latent Heat:
$$L \equiv (\partial H/\partial n)_{p,T} \qquad \text{(usually irreversible)}$$

(4) Apparent Heat Capacity:
$$C_p^{\#} \equiv dH/dT = (\partial H/\partial T)_{p,n} + (\partial H/\partial n)_{p,T}\cdot dn/dT$$

(5) Temperature-dependent Reaction Rate:
$$dn/dT = (dn/dt)/(dT/dt) \qquad (dT/dt = \text{heating rate})$$

Fig. 3 Thermodynamic equations

composition does not change, only the first term in Eq. 1 contributes to the change in enthalpy. The differential quotient is expressed by the *heat capacity*, C_p, defined by Eq. 2.

Since the 1960s, differential scanning calorimetry, DSC, has become sufficiently quantitative, to considerably increase the available heat capacity data. In the last 20 years, finally, temperature-modulated DSC, TMDSC, has become available [6, 7]. It allows to separate the reversible and irreversible contributions to C_p, as expressed by Eqs. 4 and 5, where dt represents the change in time. The apparent heat capacity, $C_p^{\#}$, is then a quantity which consists of both the reversible and irreversible contributions.

Figure 4 displays the resulting thermodynamic functions for crystalline (subscript c) and amorphous polyethylene (subscript a) [6, 7]. The data were arrived at by first measuring C_p of the amorphous melt in equilibrium. Integration of the heat capacity over temperature yields the enthalpy H_a using the Eq. 6 in Fig. 4. The measurements on samples of various crystallinities were then used to yield H_c of the crystal, which is set to 0 at 0 K by subtracting the integration constant H_c^o [22]. The curves H_c and H_a could next be connected with the Eq. 6 using the equilibrium latent heat of fusion, ΔH_f, at the equilibrium melting temperature, T_m^o, separately determined to be 4.11 kJ (mole of CH_2)$^{-1}$ and 414.6 K [23], respectively. Next, with Eq. 7 of Fig. 4, the entropy contribution was calculated and the graph completed by normalizing the free enthalpy, G, at 0 K to H_c^o making use of Eq. 8. The continuous curves represent now the integral functions of the equilibrium thermodynamics of the melt and crystal of polyethylene.

On cooling below T_m^o, polymer melts usually remain metastable for a reasonable temperature range before crystallization can be nucleated [4]. The C_p of the high-temperature portion of this non-equilibrium, supercooled liquid can be measured in the same way as that of the equilibrium melt. Beyond this range, a limited
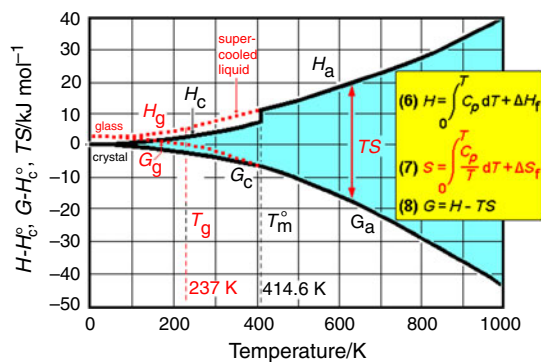
Fig. 4 The enthalpy, free enthalpy Gibbs function, and entropy contribution for equilibrium crystals (c), glass (g), and amorphous liquid (l), derived from DSC on amorphous and semicrystalline samples

extrapolation to lower temperature is possible, guided by the knowledge of the molecular motion in the melt [24]. However, as with any liquid which does not crystallize, the glass transition intervenes long before the absolute zero of temperature is reached. At T_g, the liquid changes into a solid glass as shown in Fig. 1. The thermodynamic functions of the non-equilibrium, supercooled liquid and the glass of polyethylene are indicated by the dotted lines in Fig. 4. The ATHAS Data Bank [25–35] contains information for a larger number of linear macromolecules and related compounds. These data are rarely available in standard collections of thermodynamic functions, but are vital for the description of materials that contain multiple phases of different degree of order.

The thermodynamic functions in Fig. 4 refer only to pure, amorphous, and crystalline macrophases, schematically represented by Fig. 1 and the top sketch of Fig. 2. A large number of macromolecular samples, however, are *semicrystalline*, suggested in the previous section to be a globally metastable aggregate of two or more types of phases which may be as small as nanophases. In order to describe such aggregates, the thermodynamic functions of Fig. 4 must be modified, as suggested in the center sketch of Fig. 2 and then properly added to fit the composition. Special difficulties represent the changes in the interior of the nanophases, indicated in the bottom sketch of Fig. 2.

The *microcrystals* consist most often of chain-folded lamellae, imbedded in amorphous material with molecules extending across the phase boundaries and coupling the phases. One can use the Gibbs–Thomson equation [6, 7] to calculate the lowering of the melting temperature, ΔT_m, for small volumes, V (or, in turn, calculate surface-free energies from measured ΔT_m):

$$\Delta T_m = (\sigma T_m^o A)/(\Delta h_f \rho V), \qquad (9)$$

where σ is the specific surface-free energy, T_m^o the bulk equilibrium melting temperature, A the surface area, Δh_f

the specific heat of fusion (latent heat per gram), and ρ the mass density of the crystal. Equation 9 can easily be expanded for the case of more than one specific surface-free energy covering the phase [6, 7]. For 10 nm thick, laterally large, folded-chain lamellae of polyethylene, for example, ΔT_m is 26 K [5, p. 32]. In this case, only the two fold-surfaces of the lamellae contribute significantly to the surface-free energy. Clearly, when increasing the lamellar thickness ($\ell = V/A$) beyond that of the microphase dimension, let us say to 10 μm, the lowering of the melting temperature, ΔT_m, decreases to a negligible 0.026 K. Such phase is then a macrophase, as represented in Fig. 2.

The *amorphous phases* in semicrystalline polymers were thought to be sufficiently large to be described by Fig. 4. However, DSC revealed some 30 years ago that the crystallinities calculated from the ΔC_p at the glass transition and the ΔH_f at the melting temperature did not agree. In addition, the glass transition characteristics were not that of the purely amorphous phase [36]. This observation led to the identification of a *rigid amorphous fraction*, RAF [37], a nanophase with a different glass transition, corresponding to the amorphous crystal defects [6, 38]. Semicrystalline, flexible macromolecules must, thus, be usually described as three-phase structures. Above the glass transition of the RAF, the C_p becomes similar to that of a two-phase structure and above the melting temperature, it is a single-phase.

The liquids, mesophases, and crystals of various sizes are only in thermodynamic equilibrium when they have the lowest free enthalpy, G, for the given temperature range and composition. The continuation of the thermodynamic properties below the glass transition into the non-equilibrium region, as illustrated in Fig. 4, must naturally also be altered by the effect of the surfaces, as shown in Fig. 2. The additional information can usually only be measured by turning to the time-dependent, modulated calorimetry, as is discussed in the last two Sections.

Motion in gases, liquids, solids, and mesophases

The heat content is a macroscopic measurement of the energy due to *molecular motion*. For monatomic noble gas phases, an ideal state can be identified at low pressure (when the molecules are widely separated) and at high temperature (when the kinetic energy of the molecules is high). For such a gas, the thermodynamic variables, p, V, T, n, are connected by the *ideal gas equation* written as $pV = nRT$ (where R is the universal gas constant). The kinetic energy of the three degrees of freedom of *translational motion* is easily linked to the thermodynamic energy, U ($=H - pV$):

$$\frac{1}{2} M \overline{v^2} = \frac{3}{2} RT = U, \qquad (10)$$

where M is the molar mass of the atom in question and $\overline{v^2}$ the mean-square, translational velocity, so that the left third of the equations represents the molar kinetic energy and the center, the thermodynamic equivalent. The heat capacities at constant volume and pressure are then simply:

$$C_v = (\partial U/\partial T)_v = \frac{3}{2} R; \quad C_p = (\partial H/\partial T)_p = \frac{5}{2} R. \qquad (11)$$

For more complicated molecules, Eqs. 10 and 11 need to be modified. In this case, *rotational motion* of the molecules is possible, contributing an additional $R/2$ each to C_p for the 1–3 degrees of freedom (depending on symmetry). Intramolecular *vibrational motion* adds from 0 to R per degree of freedom to C_p (divided between kinetic and potential energy). In case of possible internal rotations around covalent bonds (i.e., when the molecules is flexible at higher T), there is a change in C_p when the *torsional oscillations* change to *conformational motion* (usually there is first an increase toward R, and finally a decrease in C_p to $R/2$). The molecular motion, thus, can be divided into *small-amplitude motion* (vibrations) and *large-amplitude motion* (mainly translation, rotation, and conformational motion). Finally, a *real gas* description needs two corrections to Eq. 10. These originate from the molecular volume (being small relative to the macroscopic gas volume) and from the interaction energy between the molecules (also small, as long as the molecules are far apart and at high temperature).

This combination of thermodynamics, structure, and molecular motion of gases was developed quickly after the nature of the molecules was first understood by Dalton [39, 40]. About 100 years later, the structure of crystalline solids could be determined, mainly based on X-ray scattering experiments. Metals and simple salts proved to have a high degree of order in their crystals. For the coordination number 12 for cubic and hexagonal close-packed metals, and 6–8 for ions, Einstein assumed that the force-field of the regularly placed neighbors can be approximated to be spherical. In this case, a single vibration frequency, the Einstein function Θ_E, can represent all $3N$ possible vibrations and allows the calculation of the vibrational C_p [41]. The poor fit of this approximation at low temperatures was corrected by Debye [42]. He introduced a distribution of *skeletal vibrations*, as one knew from classical vibrations in macroscopic matter. In order to connect this distribution to the atomic structure, it was terminated when the $3N$ degrees of freedom were accounted for (at the Debye frequency, Θ_D). By the first quarter of the twentieth century, this description was refined by separating the vibrations of

more tightly bound atoms or ions as *group vibrations* [43]. Later, solids of less symmetry were described by empirically fitting the combinations of 1-, 2-, and 3-dimensional Debye functions (with the parameters Θ_1, Θ_2, and Θ_3) to the low-temperature C_p, via the Tarasov functions [44–46]. After the introduction of computers, it became possible to evaluate the heat capacity of complex solids, considering thousands of group vibration frequencies which were superimposed on a broad skeletal vibration spectrum.

Figure 5 illustrates such fit for C_p of polyethylene [48], which could then be used to generate Fig. 4. The experimental data for the crystalline polyethylene fit the vibrational C_p values up to 300 K. Up to this temperature, the energy content U (=$H - pV$) is due to vibrations only. The increase of the experimental C_p above 300 K, indicated by the shading, is caused by the beginning of the change of the torsional skeletal vibrations to *large-amplitude conformational motion* (trans–gauche interchanges).

The details about the skeletal vibrations and the large-amplitude conformational motion can be seen from molecular dynamics simulations of polyethylene-like crystals. Results of such a simulation are illustrated in Fig. 6 [49]. The coupled transverse (A), torsional (B) and longitudinal (C) vibrations are marked. The dotted center illustrates a collision of the phonons A, B, and C leading to a conformational change to a 2g1 kink defect (see [3, pp. 446–452]). This defect consists of two gauche-conformations separated by one trans-conformation. Combined, they turn the chain by 180°. The bottom scale of Fig. 6 represents the time from the beginning of adding random kinetic energy to a resting chain in the simulation. The shown defect takes about 1 ps to be created. Typical life-times of such defects are 1–3 ps. The equilibrium gauche concentration can be counted from the simulation, measured from the increase in heat capacity as seen by the shaded area in Fig. 5 and also by IR spectroscopy [50]. At 320 K, it yields an equilibrium with ¼% of gauche-conformations. Because of the short life-time, each
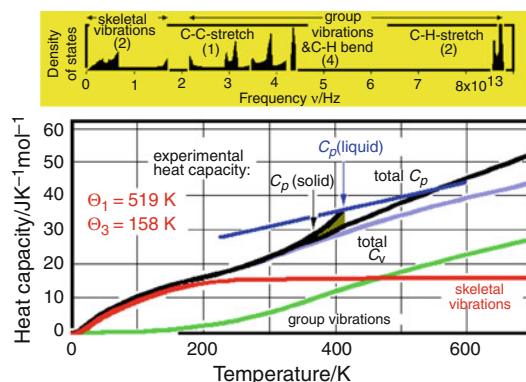
Fig. 5 Vibrational spectrum of crystalline polyethylene, represented by the upper graph [47], simplified and fitted to experimental heat capacities gained from the ATHAS effort [25–35]
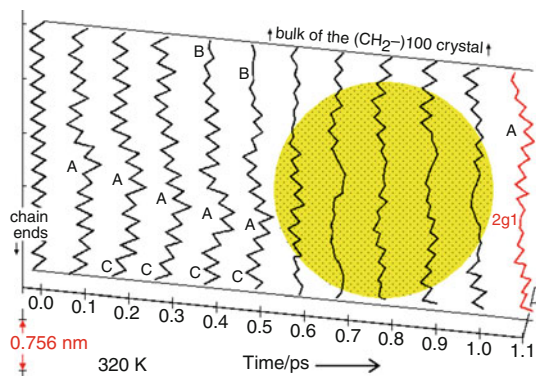
Fig. 6 Representation of the skeletal vibrations and the conformational motion by dynamic mechanical simulation [49]
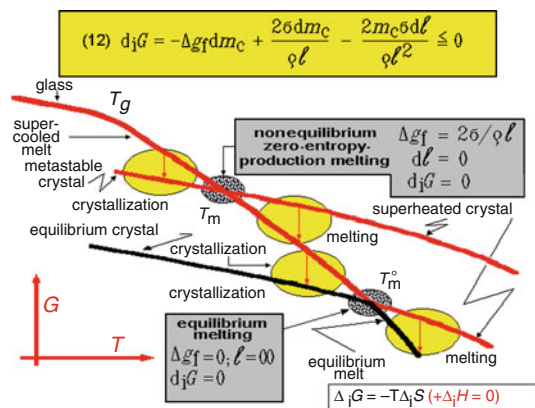

Fig. 7 Schematics of the phases

trans-conformation averages up to 10^9 changes per second. Creation and elimination of such conformational defects are also at the root of the *liquid-like motion* in crystals of flexible, linear macromolecules [49].

Turning back to Fig. 1, one can conclude that the dilute gas phase is characterized mainly by large-amplitude (translational) motion. Solids are characterized mainly by vibrational motion, but as the temperature increases, large-amplitude motions become possible, first as isolated dynamic defects, as seen in Fig. 6, later they lead to a cooperative loss of rigidity, as will be discussed below.

Equilibrium and non-equilibrium phases

The equilibrium and non-equilibrium states were introduced in Fig. 4. Non-equilibrium states are reached by hindering the transition to thermodynamically more stable states, characterized by their lower free enthalpy, G. A magnified sketch is shown in Fig. 7. It represents two equilibrium phases. One is the *melt* which changes to a non-equilibrium, supercooled liquid when hindered on crystallization with cooling. Ultimately, it becomes a solid glass at T_g. The other is an *equilibrium crystal*. It may superheat, when exceeding the equilibrium melting temperature (by insufficient time for melting). The third curve represents a *metastable microcrystal* of a fixed volume, as is described by Eq. 9. Similar sketches can be made for any of the other possible phase types, described in Fig. 1 above.

Equation 12 in Fig. 7 is based on Eq. 9, allowing changes in the mass of the crystal by melting or crystallization, dm_c, and of changes in lamellar thickness ℓ by $d\ell$. The differential d_iG is an internal free enthalpy, a *measure of irreversibility* of the transition between the two phases. The second law of thermodynamics requires d_iG to be ≤ 0 [6, 7]. The downward-pointing arrows connect two phases with such a permitted, irreversible transition.

On heating, the equilibrium crystal as well as the metastable crystal show transitions with $d_iG = 0$ when crossing the free enthalpy curve of the supercooled liquid. The first indicates the equilibrium transition, and the second, a melting without change in metastability, i.e., the crystal is just as metastable as the (supercooled) melt. This last process is called the non-equilibrium, zero-entropy-production melting and can be treated similar to equilibrium melting [6, 7].

All transitions indicated in Fig. 7 have been documented by DSC and TMDSC when carried out within a proper time scale. Equation 4 of Fig. 3 contains the time-dependent flux terms of Eq. 5, which accounts for the irreversibility of the process. For information about the temperatures where metastable phases become unstable, superfast calorimetry has become invaluable, as illustrated in [51].

Sharp and gradual transitions

In this final section, *transitions* are discussed. In Fig. 1, glass transitions and disordering transitions are shown to connect the 10 major phases of matter. The glass transitions, indicated on the left side, determine the mobile to solid transitions on cooling (upward direction in Fig. 1). The disordering transitions, indicated on the right side of Fig. 1, connect the condensed phases in the downward direction (on heating). The entropy changes on disordering allow an estimate of the change of order and type of motion for the phase transitions. Structure analyses and direct determination of molecular motion can further substantiate the nature of the transitions. The dilute gas phase, in addition, is connected to all condensed phases by evaporation (sublimation) or condensation (deposition).

Whenever a T_g intervenes on cooling of a condensed phase (upward direction in Fig. 1), there can be no further ordering. All mobile phases connect only to glasses of the same order. None of the other condensed phases can be
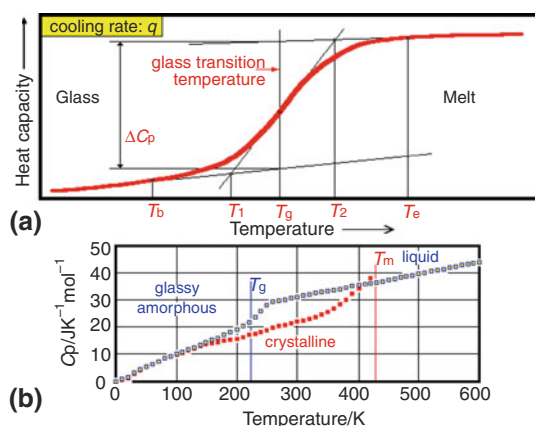
Fig. 8 The glass transition as found in typical linear, flexible macromolecules. **a** Schematic of the characteristic parameters. **b** Polyethylene, as an example of a broadened glass transition

reached directly from a glass, unless its glass transition is reversed first. The five condensed phases at the bottom can flow to some degree under a moderate stress, have varying capacity for resisting forces which tend to deform them, and under ordinary conditions, may or may not retain their size and shape. Comparing the last sentence to the dictionary descriptions of a solid given in the second section suggests that none of these phases (including the crystal) is necessarily a solid.

Figure 8 shows the change of the heat capacity during the *glass transition* of typical chain-molecules measured on cooling. Figure 8a illustrates the seven parameters which characterize a glass transition. The most quoted temperature is the mid-point of the transition, T_g. At its position, the ΔC_p is measured. The temperature difference $T_2 - T_1$ is a measure of the breadth of the transition. The beginning and end of the transition, T_b and T_e, are somewhat influenced by the precision of the C_p determination and the accuracy of the interpretation of the solid and liquid C_p, as demonstrated in Fig. 5. All five temperatures depend on the experimental time-scale and are set by the cooling rate, q. Cooling from sufficiently high temperature lets one start from an equilibrium state, ending with the specific non-equilibrium glass.

On heating, hysteresis effects due to the history of the sample are superimposed on the transition The history is set by different cooling rates, aging, annealing, or sample deformation (by drawing or compression). It can be assessed, for example, by measurement at different time scales or by controlled changing of the thermal history. All temperatures in Fig. 8a are, thus, rate dependent. For a "sharp" glass transition, as, for example, in atactic polystyrene, $T_2 - T_1$ is approximately 3–5 K [6, 7]. Detailed analyses of the calorimetry and kinetics of the glass transition by DSC [52, 53] and TMDSC [54–59] were made,

for example, for polystyrene and poly(ethylene terephthalate). For these polymers, T_g, was calculated to change by 20 K when changing the time of measurement by three orders of magnitude. A simple description of the motion involved in the glass transition was approximated earlier by the *hole model* of the liquid state, as described in [53, 60, 61].

The *broadening of the glass transition* of polyethylene, seen in Fig. 8b, was linked to the beginning of local conformational, large-amplitude motion [62]. This motion has been documented also in crystalline polyethylene as shown in Fig. 6. The isolated, large-amplitude motion for glassy polyethylene begins at about 120 K. This motion changes to a cooperative motion involving neighboring locations at about 220 K. It leads to a T_g of 237 K and a T_2 of 250 K. In semicrystalline polyethylene, the beginning of the large-amplitude motion changes with crystal perfection. At a crystallinity of 75%, it begins at 270 K, and at higher temperatures, it overlaps with the beginning of crystal melting and reorganization [63].

The broadening of the glass transition may also have other causes. Most prominent is a linking to non-randomly occurring chemical structures along the polymer chains. Multi-phase aggregates which are coupled with strained molecules crossing their interfaces can also broaden and/or shift glass transitions. Finally, samples prohibited from relaxing mechanical strains applied during cooling through the glass transition will also have a changed glass transition range. Such changes in the glass transitions and their temperature ranges have been observed in polymer solutions, copolymers, semicrystalline materials of small phase sizes, compressed samples, and drawn fibers and films. All have distinct signatures of symmetric or asymmetric broadening of the glass transition region and/or shifts in T_g. The broadening can lead to values of $T_2 - T_1$ above 100 K [6, 7], and the shift may reach temperatures above the melting transition [38]. Such broadened transitions are best established by quantitative comparison of the measured C_p with separately evaluated C_p of the solid (caused by vibrations only) and liquid (with cooperative, large-amplitude motion under equilibrium conditions). A large volume of such information is collected in the ATHAS Data Bank [25–35]. Finally, coupling across phase boundaries of semicrystalline polymers may produce nanophases of the RAF which are fully separated from the (broadened) glass transition of any remaining bulk-amorphous phase. Because of the small volume affected by the isolated large-amplitude motion (see Fig. 6), the study of the glass transition is a sensitive probe to follow the large-amplitude molecular motion and the changing of the phase structure.

In order to discuss the *order–disorder transitions* in Fig. 1, one can look at the apparent heat capacity, $C_p^{\#}$, as
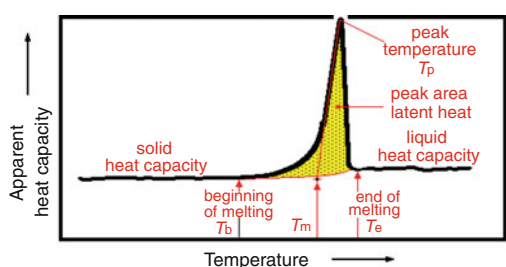
Fig. 9 The disordering transition of a typical semicrystalline polymer (melting). The seven characteristic parameters are listed

expressed by Eq. 4. Figure 9 gives a schematic of a DSC trace as obtained for a typical, semicrystalline polymer. Only when all parameters are evaluated, is the description adequate. Well-crystallized, the melting endotherm may be only 3–5 K wide. This is sufficiently broad so that instrument-lag is of little influence and can be corrected for. Calibrations of the lag are always necessary to refine the results. The peak temperature (corrected for instrument-lag) is then indicating the maximum rate of melting and the extrapolation of the linear portion of the melting peak yields the melting temperature, T_m. The beginning of melting is influenced by impurities, low molar mass content, and poorly crystallized portions of the sample.

The major change of $C_p^\#$ on melting is proportional to the integral latent heat absorbed up to the temperature of interest. The measured ΔC_p, separating the levels of the thermodynamic C_p(solid) and C_p(melt, liquid) can then be considered to signify a "glass transition." Commonly this change of C_p is called the "baseline," marked as the thin line in Fig. 9. If the progress of the change in ΔC_p is governed fully by the progress of melting, the glass transition is forced by the melting, having been shifted to coincide with the melting transition because of the better packing in the crystal. If this is not the case, the "solidity" of the crystal is lost before melting and there is a separate glass transition [64].

Must a crystal always be a solid? The answer to this question was found at the end of our 50-year quest to understand the phases of matter. Diamond, a rigid macromolecule, for example, has a strong network of covalent bonds, allowing vibrational motion only. Large-amplitude motion in form of rotation of small portions of the phase about appropriate bonds becomes possible only by simultaneous bond breakage. This leads at atmospheric pressure and elevated temperature to a change of the metastable diamond to the stable graphite. Melting can occur only under an appropriately high pressure and temperature. The melting range is at 3–4000 K, but accompanied by

considerable sublimation. Looking at metals, many of them are ductile, i.e., they do not resist forces strongly which tend to deform them. Lead is one of the ductile metals which needs only weak forces to deform. Many small, flexible molecules produce outright soft crystals, such as paraffins. The proof of the boxed statement in Fig. 9 was found when studying crystals of flexible linear macromolecules like POE, poly(oxyethylene), and nylon, aliphatic poly(amide). Without changing its crystal structure, POE and some nylons attain liquid-like local molecular mobility and on heating, the liquid C_p is reached below the melting temperature. High molar mass PEO crystals have a glass transition of 324 K and melt at 341 K [65]. The triclinic nylon 6.6 crystals have a glass transition at 409 K, a disordering transition (Brill transition) to the hexagonal condis-crystal at 455 K, and a final melting at 525 K. Lower-melting nylons may not undergo the transition to a condis-phase, but possess a full or partial glass transition before melting [66].

Similar to the broadening of the glass transition, semi-crystalline polymers may have *broadened disordering transitions*, measurable by the absorption of latent heat (entropy) over a wide temperature range. If the phases in the schematic of Fig. 1 are linked by such broadened disorder transitions, the classical system of first-order and higher-order phase transitions proposed by Ehrenfest [11] are not of universal use. As a consequence, the free enthalpy schematic of Fig. 7 with its sharp intersections of the phase lines is also only an approximation.

The separation of reversible and irreversible changes in enthalpy is based on the equations in Fig. 3, whenever possible, using the zero-entropy production paths suggested in Fig. 7. The various modes of DSC, TMDSC, and fast calorimetry are the tools for such measurements [6, 7]. Ordering transitions are more difficult to analyze. They are often irreversible because of the hindering of the transition due to crystal or molecular nucleation and incomplete transformation [4, 5]. Figure 10 illustrates a typical analysis of a multi-phase system with broadened glass transitions as well as broadened ordering and disordering transitions.

The experiment of the quenched poly(butylene terephthalate), PBT, starts with the recording of the standard DSC plot of C_p versus T, the bottom curve in Fig. 10. Next, the heat capacity of the solid and liquid needs to be entered. If not already known from the ATHAS Data Bank [25–35], these must be measured separately and analyzed, as shown for polyethylene with Figs. 4 and 5. This is a major undertaking, but without it, the following quantitative analysis is limited to estimates which may have large errors. Then, the TMDSC results are to be added into Fig. 10, as shown in the upper curve. From the ΔC_p, measured by TMDSC, a mobile amorphous fraction, w_a, is
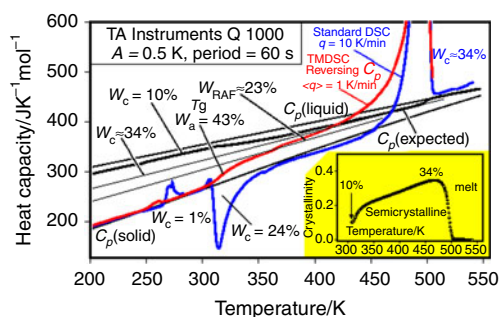
$$(13)\ C_p(\text{apparent})=(w_c+w_{RAF})C_p(\text{solid})+(1-W_c-W_{RAF})C_p(\text{liquid})-\frac{dw_c}{dT}\Delta H_f(T)$$

Fig. 10 Quantitative thermal analysis of poly(butylene terephthatate) with 10% microphase crystals, 43% mobile amorphous microphases, MAF, and 23% RAF nanophases [51]

calculated at its T_g. This leads to the first quantitative answer. The ΔC_p requires a 43% liquid sample above the glass transition. The expected heat capacity for a 57% solid sample can now be drawn into Fig. 10 (the lower of the two thin, straight lines). Obviously, it agrees with the experiment only over the short temperature range to about 350 K. The preliminary interpretation based on these data is as follows: the standard DSC has some unknown irregularities at about 275 K (a), a cold crystallization exotherm, starting at the beginning of the glass transition (b), a too low C_p above 350 K before the large endotherm (c), and the expected C_p beyond the melting endotherm (d).

Points (a)–(d) need now to be clarified [51]. Point (a) initially remained open, but could later be identified as an instrumental artifact created during the thermal pretreatment of the sample [67]. The cold crystallization exotherm (b) to 350 K accounts only for about 10% crystallinity, w_c. The much larger endotherm with a maximum close to 500 K should account for the final crystallinity, i.e., the crystallinity of the quenched starting material plus the result from the cold crystallization exotherm. Before this endotherm can be evaluated, a quantitative baseline must be established. From separate experiments with annealed samples, it was found that there is a rigid amorphous fraction, RAF, with a glass transition at 375 K and an upper end at about 400 K. At this upper end of the T_g(RAF), the sample can be represented by only two phases, the microphase of crystals and two now fully mobile amorphous phases. Assuming a similar temperature range of the glass transition of the RAF of the annealed and quenched samples, one can find a maximum w_c of 34%, a RAF of 23%, and a MAF of 43%. With Eq. 13 of Fig. 10 a unique, expected baseline C_p(expected) can be calculated with a linearly variable w_{RAF}, as indicated in the figure. The exotherm and endotherm yield the changing crystallinity of the quenched sample on heating, as given by the insert of Fig. 10. The initial crystallinity of the quenched sample is 10%, it increases with the cold

crystallization exotherm (b) to $w_c = 20\%$. The continuing, low baseline (c) is due to further crystallization, reaching a maximum of $w_c = 34\%$ before the subsequent melting reduces it to zero. The final melting (d) begins at 420–440 K with an excess of irreversible melting, separable with Eqs. 1–5. Assuming only lamellar crystals, the surface properties can be evaluated with Eq. 9. Additional details about reversibility are available through quasi-isothermal TMDSC and fast DSC [51]. Only when all of these changes in structure and mobility are known over the broad, overlapping transition ranges, one can optimize the processing conditions and suggest samples with the best properties for a chosen application.

Conclusions

An up-to-date thermodynamic description of the condensed phases is not possible when being limited to the presently still widely accepted historically developed ideas. A consistent set of improved definitions and descriptions has been developed over the last 50 years and is outlined. The conclusion is that one can classify a phase as consisting of one of three types of molecules, one of nine different condensed phases, and one of three phase sizes. This system leads to operational definitions of 57 different classes of materials. As indicated in Fig. 1, the different materials are uniquely linked by two types of phase transitions, the glass transitions and the disorder transitions. The glass transitions set the temperature of solidification, i.e., are linked to the mechanical appearance of the phases, while the disorder transitions are linked to their physical structures. All can be analyzed and understood by quantitative thermal analysis, supported by microscopic measurements of structure and molecular motion. Key is the possibility to distinguish between solids and fluids by measuring the glass transition temperature, T_g. This led to the conclusion that (in rare cases) even crystals may change from solid to liquid behavior below their melting temperature. Few of the studied examples have transitions as required by the idealized "orders of transition," and rarely any of the known materials have been analyzed to the limits possible by present-day calorimetry. A large amount of work needs still to be done before the structure–property correlation is fully understood, particularly for the modern materials containing nanophases.

References

1. Chen W, Wunderlich B. Nanophase separation of small and large molecules. Macromol Chem Phys. 1999;200:283–311.
2. Wunderlich B. Thermodynamics and properties of nanophases. Thermochim Acta. 2009;492:2–15.

3. Wunderlich B. Macromolecular physics, vol. 1. Crystal structure, morphology, defects. New York: Academic Press; 1973. A PDF reprint, fully electronically searchable with a new Preface has been published in 2005 and is now available as part of [6] and [7], and via www.scite.eu.

4. Wunderlich B. Macromolecular physics, vol. 2. Nucleation, crystallization, annealing. New York: Academic Press; 1976. A PDF reprint, fully electronically searchable with a new Preface has been published in 2005 and is now available as part of [6] and [7], and via www.scite.eu.

5. Wunderlich B. Macromolecular physics, vol 3. Crystal melting. New York: Academic Press; 1980. A PDF reprint, fully electronically searchable with a new Preface has been published in 2005 and is now available as part of [6] and [7], and via www.scite.eu.

6. Wunderlich B. Thermal analysis of polymeric materials. Berlin: Springer; 2005.

7. Wunderlich B. Thermal analysis of materials; 2007. http://athas.prz.rzeszow.pl, www.scite.eu, or http://www.evitherm.org/index.asp.

8. Merriam Webster's Collegiate Dictionary, 11th ed. Springfield, MA: Merriam-Webster Inc.; 2003. http://www.m-w.com.

9. Bridgeman PW. The logic of modern physics. New York: MacMillan; 1927.

10. Wunderlich B. A classification of molecules and transitions as recognized by thermal analysis. Thermochim Acta. 1999;340(/41): 37–52.

11. Ehrenfest P. Phase changes in the ordinary and extended sense classified according to the corresponding singularities of the thermodynamic potential. Proc Acad Sci Amsterdam 1933;36: 153–157. Suppl 75b, Mitt Kammerlingh Onnes Inst, Leiden.

12. Quoted from [6] based on standard texts and the early discussions on the equilibrium of heterogeneous Substances in 1875 and 1877 by Gibbs JW, see [13].

13. A reprint of the papers by Gibbs JW from the Trans Conn Acad III (1875; 76: 108–248 and 1877; 78, 343–524) can be found in: Bumstead HA, van Name RG. The scientific papers of J. Willard Gibbs, vol 1. Thermodynamics. New York: Dover Publications; 1961.

14. Wunderlich B, Grebowicz J. Thermotropic mesophases and mesophase transitions of linear, flexible macromolecules. Adv Polym Sci. 1984;60/61:1–59.

15. Wunderlich B, Möller M, Grebowicz J, Baur H. Conformational motion and disorder in low and high molecular mass crystals. Berlin: Springer; 1988. (Adv Polym Sci, vol 87).

16. Hill TL. Thermodynamics of small systems, parts I and II. New York: Benjamin; 1963/1964 (combined reprint of both parts, New York: Dover; 1994).

17. Quoted from the transcript of the lecture at the 1959 annual meeting of the American Physical Society. http://www.its.caltech.edu/~feynman/plenty.html.

18. Hosemann R. Crystalline and paracrystalline order in high polymers. J Appl Phys. 1963;34:25–41.

19. Wunderlich B, Poland D. Thermodynamics of crystalline linear high polymers. II. The influence of copolymer units on the thermodynamic properties of polyethylene. J Polym Sci A. 1963; 1:357–72.

20. The term 'macromolecule' was first used on p. 788 of Staudinger H, Fritschi J. Über die Hydrierung des Kautschuks und über seine Konstitution. Helv Chim Acta 1922; 5: 785–806.

21. In his Nobel Lecture of 1953, Staudinger sets the limit of small molecules at 1,000 atoms (Staudinger H. Arbeitserinnerungen. Heidelberg: Hüthig; 1961, p. 317).

22. Wunderlich B. Motion in polyethylene. I. Temperature and crystallinity dependence of the specific heat. J Chem Phys. 1962; 37:1203–7.

23. Wunderlich B, Czornyj G. A study of equilibrium melting of polyethylene. Macromolecules. 1977;10:906–13.

24. Pyda M, Wunderlich B. Analysis of the residual entropy of amorphous polyethylene at zero kelvin. J Polym Sci B. 2002;40: 1245–53.

25. Gaur U, Shu H-C, Mehta A, Wunderlich B. Thermodynamic properties of linear macromolecules, part I. Selenium. J Phys Chem Ref Data. 1981;10:89–117.

26. Gaur U, Wunderlich B. Thermodynamic properties of linear macromolecules, part II. Polyethylene. J Phys Chem Ref Data. 1981;10:119–52.

27. Gaur U, Wunderlich B. Thermodynamic properties of linear macromolecules, part III. Polyoxides. J Phys Chem Ref Data. 1981;10:1001–49.

28. Gaur U, Wunderlich B. Thermodynamic properties of linear macromolecules, part IV. Polypropylene. J Phys Chem Ref Data. 1981;10:1051–64.

29. Gaur U, Wunderlich B. Thermodynamic properties of linear macromolecules, part V. Polystyrene. J Phys Chem Ref Data. 1982;11:313–25.

30. Gaur U, Lau S-F, Wunderlich B. Thermodynamic properties of linear macromolecules, part VI. Acrylic polymers. J Phys Chem Ref Data. 1982;11:1065–89.

31. Gaur U, Wunderlich BB, Wunderlich B. Thermodynamic properties of linear macromolecules, part VII. Other carbon backbone polymers. J Phys Chem Ref Data. 1983;12:29–63.

32. Gaur U, Lau S-F, Wunderlich BB, Wunderlich B. Thermodynamic properties of linear macromolecules, part VIII. Polyesters and polyamides. J Phys Chem Ref Data. 1983;12:65–89.

33. Gaur U, Lau S-F, Wunderlich B. Thermodynamic properties of linear macromolecules, part IX. Aromatic and inorganic polymers. J Phys Chem Ref Data. 1983;12:91–108.

34. Varma-Nair M, Wunderlich B. Thermodynamic properties of linear macromolecules, part X. Update of the *ATHAS* 1980 data bank. J Phys Chem Ref Data. 1991;20:349–404.

35. The updated ATHAS Data Bank is available also on the internet through Pyda M. http://athas.prz.rzeszow.pl.

36. Menczel J, Wunderlich B. Heat capacity hysteresis of semicrystalline macromolecular glasses. J Polym Sci Polym Lett Ed. 1981;19:261–4.

37. Suzuki H, Grebowicz J, Wunderlich B. The glass transition of polyoxymethylene. Br Polym J. 1985;17:1–3.

38. Wunderlich B. Reversible crystallization and the rigid amorphous phase in semicrystalline macromolecules. Prog Polym Sci. 2003;28: 383–450.

39. Dalton J. A new system of chemical philosophy. London: Macmillan; 1808 (The idea about the atomic nature of matter appeared first in his notebook covering 1802/04, see also [40]).

40. The Ref. [39] is frequently reprinted; for example, see: The science classical library. New York: The Citadel Press; 1964.

41. Einstein A. Planck's theory of radiation and the theory of specific heat. Ann Phys. 1907;22:180–190, 800.

42. Debye P. Concerning the theory of specific heat. Ann Physik. 1912;39:789–839.

43. Schrödinger E. Thermische Eigenschaften der Stoffe. In: Geiger H, Scheel K, Henning F, editors. Handbuch der Physik, vol. 10. Berlin: Springer; 1926. p. 275.

44. The original paper on the development and application of the Tarasov function is: Tarasov VV. Theory of the heat capacity of chain and layer structures. Zh Fiz Khim 1950; 24: 111–128; see also [45, 46].

45. Tarasov VV. Heat capacity of chain and layer structures. Zh Fiz Khim 1953; 27: 1430–1435; see also [44, 46].

46. Tarasov VV, Yunitskii GA. Theory of heat capacity of chain-layer structures. Zh Fiz Khim 1965; 39; 2077–2080; see also [44, 45].

47. Barnes J, Fanconi B. Critical review of vibrational data and force field constants for polyethylene. J Phys Chem Ref Data. 1978; 7: 1309–21.

48. A first analysis of the heat capacity of crystalline polyethylene and tables of one dimensional Debye functions for the evaluation of the Tarasov function are available in [22].

49. Sumpter BG, Noid DW, Liang GL, Wunderlich B. Atomistic dynamics of macromolecular crystals. Adv Polym Sci. 1994; 116:27–72.

50. Wunderlich B, Pyda M, Pak J, Androsch R. Measurement of heat capacity to gain information about time scales of molecular motion from Pico to Megaseconds. Thermochim Acta. 2001;377: 9–33.

51. Pyda M, Nowak-Pyda E, Heeg J, Huth H, Minakov AA, Di Lorenzo ML, Schick C, Wunderlich B. Melting and crystallization of poly(butylene terephthalate) by temperature-modulated and super-fast calorimetry. J Polym Sci B Polym Phys. 2006;44:1364–77.

52. Wunderlich B, Bodily DM. Dynamic differential thermal analysis of the glass transition interval. J Polym Sci C. 1964;6:137–48.

53. Wunderlich B, Bodily MH, Kaplan MH. Theory and measurements of the glass-transformation interval of polystyrene. J Appl Phys. 1964;35:95–102.

54. Boller A, Schick C, Wunderlich B. Modulated differential scanning calorimetry in the glass transition region. Thermochim Acta. 1995;266:97–111.

55. Wunderlich B, Boller A, Okazaki I, Kreitmeier S. Modulated differential scanning calorimetry in the glass transition region, part II. The mathematical treatment of the kinetics of the glass transition. J Therm Anal. 1996;47:1013–26.

56. Boller A, Okazaki I, Wunderlich B. Modulated differential scanning calorimetry in the glass transition region, part III. Evaluation of polystyrene and poly(ethylene terephthalate). Thermochim Acta. 1996;284:1–19.

57. Thomas LC, Boller A, Okazaki I, Wunderlich B. Modulated differential scanning calorimetry in the glass transition region, part IV. Pseudo-isothermal analysis of the polystyrene glass transition. Thermochim Acta. 1997;291:85–94.

58. Okazaki I, Wunderlich B. Modulated differential scanning calorimetry in the glass transition region, part V. Activation energies and relaxation times of poly(ethylene terephthalate). J Polym Sci B Polym Phys. 1996;34:2941–52.

59. Okazaki I, Wunderlich B. Modulated differential scanning calorimetry in the glass transition region, part VI. Model calculations based on poly(ethylene terephthalate). J Therm Anal. 1997;49: 57–70.

60. Eyring H. Viscosity, plasticity and diffusion as examples of absolute reaction rates. J Chem Phys. 1936;4:283–91.

61. Hirai N, Eyring H. Bulk viscosity of liquids. J Appl Phys. 1958; 29:810–6.

62. Gaur U, Wunderlich B. The glass transition temperature of polyethylene. Macromolecules. 1980;13:445–6.

63. Wunderlich B, Sullivan P, Arakawa T, DiCyan AB, Flood JF. Thermodynamics of crystalline linear high polymers. III. Thermal breakdown of the crystalline lattice of polyethylene. J Polym Sci A. 1963;1:3581–96.

64. Wunderlich B. The glass transition of polymer crystals. Thermochim Acta. 2006;446:128–34.

65. Qiu W, Wunderlich B. Reversible melting of high molar mass poly(oxyethylene). Thermochim Acta. 2006;448:136–46.

66. Wunderlich B. Thermal properties of aliphatic nylons and their link to crystal structure and molecular motion. J Therm Anal Calorim. 2008;93:7–17.

67. Chen H, Cebe P. Quenching of polymer inside aluminum DSC pans: origin of an apparent artifact. Thermochim Acta. 2008;476: 63–5.